Hindawi
Advances in Materials Science and Engineering
Volume 2023, Article ID 9759187, 1 page
https://doi.org/10.1155/2023/9759187

Retraction

Retracted: Optimization of Process Parameter on AA8052 Friction Stir Welding Using Taguchi's Method

Advances in Materials Science and Engineering

Received 26 December 2023; Accepted 26 December 2023; Published 29 December 2023

This article has been retracted by Hindawi, as publisher, following an investigation undertaken by the publisher [1]. This investigation has uncovered evidence of systematic manipulation of the publication and peer-review process. We cannot, therefore, vouch for the reliability or integrity of this article.

Please note that this notice is intended solely to alert readers that the peer-review process of this article has been compromised.

Wiley and Hindawi regret that the usual quality checks did not identify these issues before publication and have since put additional measures in place to safeguard research integrity.

We wish to credit our Research Integrity and Research Publishing teams and anonymous and named external researchers and research integrity experts for contributing to this investigation.

The corresponding author, as the representative of all authors, has been given the opportunity to register their agreement or disagreement to this retraction. We have kept a record of any response received.

References

[1] P. Sharma, S. Baskar, P. Joshi et al., "Optimization of Process Parameter on AA8052 Friction Stir Welding Using Taguchi's Method," *Advances in Materials Science and Engineering*, vol. 2022, Article ID 3048956, 8 pages, 2022.

Hindawi
Advances in Materials Science and Engineering
Volume 2022, Article ID 3048956, 8 pages
https://doi.org/10.1155/2022/3048956

Research Article

Optimization of Process Parameter on AA8052 Friction Stir Welding Using Taguchi's Method

Pankaj Sharma,[1] S. Baskar,[2] Puneet Joshi,[3] T. A. Raja,[4] Santosh Kumar Sahu,[5] Medapati Sreenivasa Reddy,[6] and M. Rudra Naik[7]

[1]*Department of Mechanical Engineering, JECRC University, Jaipur, India*
[2]*Centre for Excellence in Energy and Nano Technology, S.A. Engineering College, Chennai 600077, India*
[3]*Department of Electrical Engineering, Rajkiya Engineering College, Ambedkar Nagar, Uttar Pradesh 224122, India*
[4]*Department of Agricultural Statistics & Economics, Sher-e-Kashmir University of Agricultural Sciences and Technology, Srinagar, Jammu and Kashmir 190025, India*
[5]*Department of Mechanical Engineering, Veer Surendra Sai University of Technology, Burla, Odisha 768018, India*
[6]*Department of Mechanical Engineering, Aditya Engineering College, Surampalem 533437, East Godavari District, Andhra Pradesh, India*
[7]*Department of Electro-Mechanical Engineering, Arba Minch University, Sawla Campus, Arba Minch, Ethiopia*

Correspondence should be addressed to M. Rudra Naik; rudra.naik@amu.edu.et

Received 5 April 2022; Accepted 4 May 2022; Published 14 June 2022

Academic Editor: K. Raja

The Taguchi method of experimental design was employed in this study to scrutinize the impact of welding processing factors, including rotating speed, travelling speed, and pin profile on ultimate tensile strength, microhardness, and impact strength of the Friction Stir Welded AA 8052 joint. The S/N values for each process specification were calculated using an orthogonal array of L9 design. The 1150 rpm and 28.5 mm/min were the greatest tensile strength, microhardness, S/N evaluation parameters, respectively, and a used cylinder pin. A combination of 1150 rpm and 32.5 mm/s and a conical cylindrical pin provided the best impact toughness results. According to the analysis of variance, the spinning speed, travel feed, and pin shape had a 37.34% impact on ultimate strength and a further 34.33% impact on microhardness. A second set of tests verified the findings, with tensile strength of 349.96 MPa, hardness of 115.31 H, and impact strength of 7.95 kJ.

1. Introduction

Light aluminum alloy welding has always been a difficult task for designers, producers, and technicians alike [1]. High thermal buildings, such as a high thermal growth coefficient, high thermal conductivity, greater oxidation, and concretion contractions, as well as a developed solubility of hydrogen and other gasolines in the molten stage, provide several obstacles for the joining process [2, 3]. Hot cracking occurs in the weld zone (dissolved region) due to the dispersion of alloying elements through compaction, which reverses the heat process influence and generates an extremely crude microstructure, leading in poor mechanical qualities of a joint [4]. The welding framework may be utilized in the aircraft industry to reduce the amount of light we consume [5].

For nonconsumable devices, friction stir weld can be utilized to solder a most difficult creation than the bottom material. As a joining invention for metal joints, friction stir weld has various advantages, including the elimination of faults such porosity and insufficient blend and filler materials, which decreases manufacturing costs [6, 7]. The mechanical qualities of friction stir weld of Al and its own combinations are superior to those of ordinary fusion welds since the joints are defect-free [8]. Friction stir weld processing stipulations on microstructure growth have been the subject of numerous studies and comparisons between friction stir weld and standard blend methods such as TIG

and MIG connected Al composites structures have been thoroughly examined [9, 10]. To ensure high-quality joined junctions, friction stir weld relies on shared plan and source geometry of equipment [11]. This is because these specifications have a significant impact on heat flow and product flow design, as well as on the creation of microstructures [12]. Many published papers have looked at the effects of friction stir weld guidelines on the metallurgical and mechanical characteristics of various low weight aluminum alloy junctions [13, 14]. Only a few research studies have focused on formalizing and optimizing the influence of Friction stir weld handing out conditions on the metallurgic and mechanical characteristics of alike and distinct aluminum joints. The Taguchi method of experimentation methodology is beneficial for optimizing the parameters of the procedures. In addition, it demonstrates how well each parameter contributes to the overall goal of the process. For example, upright pressure has a greater impact on joint tensile strength than any of the other three welding criteria in friction stir weld of A319 directed alloy (travel velocity, rotating speed, and vertical centre force), whereas a few papers have shown that spinning speed has the greatest impact on joint tensile strength over both vertical pressure and travel speed [15]. Moreover, the formalization and optimization of welding standards will also reduce the cost of welding processes for both identical and different Al alloys joints, in addition to being more convenient [16–18]. These parameters were tested on AA8052 metals to see if they affected the flexibility, solidity, impact stamina, and superior disorder in the abrasion mix assembly process for 8052 joints, and the results showed that they had a significant effect in all of those areas [19]. Using orthogonal array design, the process parameters, rotating speed, travel speed, and pin shape, are fine tuned for finding ultimate tensile strength, microhardness, and impact strength of AA8052 material joints.

2. Experimental Procedure

In order to build the structure, we used AA8052 alloy plates of 5 mm thickness. Corrosion-resistant 8052 alloy is an excellent choice for big maritime buildings, such as tanks for LNG ships, since it is very resistant to saltwater and salt spray. The 100 mm × 60 mm partitions of the aluminum 8052 lightweight plates were actually used. The tool's rotational speed (950, 1150, and 1450 rpm) and 26, 32.5, and 41 travel speed (mm/min) are used as welding recommendations. FSW (square butt joint) joints were formed using an H13 steel welding tool with pins made up cylinder pin with flutes, con, and triangular pins. Table 1 shows the FSW factors and strategy levels.

The FSW factors of AA 8052 metals were improved using Taguchi's L9 orthogonal array of practices. Rotating speed (W), travel feed (V), and tool geometry were chosen as the FSW guidelines for this study. Strength, hardness, and impact resistance are all output properties. Analysis of the sound-to -noise ratio was carried out for each and every procedure criterion. Use of signal-to-noise analysis helped to keep desired features as stable as possible. This resulted in more accurate and similar values for ultimate tensile strength, impact strength, and hardness [20]. To advance the mechanical of joints for certain alloys, this study sets out to conduct experiments. Formula (1) was employed to compute the S/N ratio, which displays the quality attributes:

$$\frac{s}{y} = -10 \log\left(\frac{1}{n}\sum_{l=1}^{R}\frac{1}{y_i^2}\right). \quad (1)$$

By employing Taguchi's L9 orthogonal array of methods, we were able to enhance the FSW properties of aluminum 8052. Device pin geometry and rotational speed (W) were used as the FSW criteria for this study. Output qualities include hardness, elasticity, and abrasion resistance. For each and every method criterion, the S/N (signal-to-noise ratio) was evaluated [21, 22]. Stability was maximized through the application of signal-to-noise analysis. More precise and comparable data for UTS, impact strength, and hardness were obtained as a result of this process. This study sets out to undertake experiments in order to enhance the mechanical characteristics of joints for certain alloys. Utilizing formula (1), the S/N ratio was calculated, which shows the quality characteristics.

3. Results and Discussion

3.1. Ultimate Tensile Strength. The highest attainable UTS was 352.49 MPa for practice 4 (1150 rpm, 26 mm/min). In addition, for an example prepared from the weld problem in Experiment 9 (1450 rpm, 41 mm/min, triangular pin), the lowest UTS. There was a weld zone fracture in all of the samples. Table 2 shows the results of tensile testing.

3.2. Analysis of Sound-to-Noise Ratio. By this analysis, the ultimate tensile strength of a residential property was examined as one of the factors that affect the FSW. Alloy FSW junction tensile strength was a primary objective in this investigation [23]. With the "far higher is actually much better" premise in mind, the goal is to have the highest possible UTS values for all variables. Using L9 orthogonal selection design less weight aluminum alloy 8052 joints, the S/N ratio of corresponding studies is shown in Table 3. The welding example was the only one to fail the tensile test.

If the signal-to-noise ratio is higher, the FSW process will be more effective. As a result, the most model S/N really worth is the optimal level of processing requirements. Consequently, 1150 rpm rotational speed, 26 mm/min travel speed, and CWF resource pin geometries are the optimal levels of the process criteria. In Figure 1, the S/N ratio gives the most important role.

Figure 1 shows that the sound-to-noise ratio of spinning speed rises between 950 rpm and 1150 rpm and subsequently falls between 1150 rpm and 1450 rpm, indicating that the optimal rotating speed is in fact 1150 rpm. Sound-to-noise ratio of welding travelling speed drops between 26 mm/min and 32.5 mm/min and then rises from 32.5 to 41 mm/min; thus, the ideal welding speed is 41.5. As shown by the S/N ratio data obtained from the resource pin profile page, the

Table 1: FSW factors and strategy levels.

S. No.	Factors code	Level 1	Level 2	Level 3
1	Rotating speed (W) (rpm)	950	1150	1450
2	Travelling speed (V) (mm/min)	26	32.5	41
3	Tool geometry	Cylinder pin with flutes (CWF)	Tapered cylinder pin profile (Con)	Triangular pin profile (TRI)

Table 2: Results of tensile testing.

S. No	Rotational speed (W)	Travel speed (V)	Tool geometry	Ultimate tensile strength (UTS) (MPa)
1	950	26.0	CWF	344.24
2	950	32.5	Con	313.72
3	950	41.0	TRI	327.52
4	1150	2560	CWF	352.49
5	1150	32.5	Con	320.04
6	1150	41.0	TRI	335.28
7	1450	26.0	CWF	330.38
8	1450	32.5	Con	327.19
9	1450	41.0	TRI	306.44

Table 3: S/N ratio of AA8052 joints.

S. no	Rotational speed (W)	Travel speed (V)	Tool geometry	Ultimate strength (MPa)	Tensile ratio
1	950	26.0	CWF	345	50.7701
2	950	32.5	Con	314	49.9453
3	950	41	TRI	328	50.2386
4	1150	26.0	CWF	353	50.8785
5	1150	32.5	Con	320	50.1329
6	1150	41.0	TRI	335	50.5264
7	1450	26.0	CWF	330	50.3164
8	1450	32.5	Con	327	49.6621
9	1450	41.0	TRI	306	49.8851

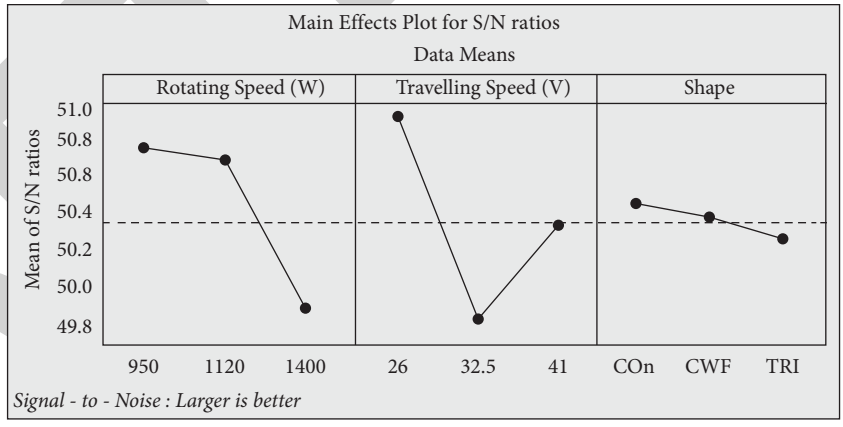

Figure 1: Main effects plot on sound-to-noise ratio.

FSW joint is substantially more durable when it is supported by cylinder pins with flues.

3.3. ANOVA. The influence of each process parameter was studied using ANOVA. It evaluates a set of experimental data is impacted by various operational conditions. NOVA is active to examine the impact of distinct course principles on the UTS of a material [24]. Using the F-test, the quantity of each weld parameter that affects the UTS of a 8052 aluminum metals junction is shown in Table 4.

In Table 4, the P market value directs the possibility of uncontrollability of processing conditions, whereas the F market value shows the amount of relationship between manageable process requirements and optimal ultimate

Table 4: Analysis of variance for mean.

Source	DF	Adj SS	Adj MS	*F*-test	*P*
Rotating speed	2	0.47946	0.239722	37.32	0.027
Travelling speed	2	0.83328	0.416592	64.85	0.016
Tool pin profile	2	0.01456	0.007268	1.14	0.468
Error	2	0.01286	0.006426		
Total	8	1.34002			

tensile strength [25]. It is chosen to have the highest possible *F* value, the lowest possible *P* value, and the factor that has a 5% chance of occurring as an important constraint for a better joint quality. The rotating speed contributes 37.34% to the trip speed, while the pin geometry accounts for 13% of the travel speed. Together, these two factors account for 64.86% of the travel speed. So, it is apparent that travel speed is the most significant factor in maximizing ultimate tensile strength.

3.4. Weld Zone's Hardness. Table 5 summarizes the results of measuring the microhardness of the AA8052 welded connections with a micro-Vickers hardness tester. According to this data, the sample of the eighth practice (1450 rpm, 32.5 mm/min) had the greatest microhardness of 117.

3.5. Analysis of Sound-to-Noise Ratio. During this specific investigation, microhardness was measured to be one of the most desirable unique features that were used to optimize the constraints of FSW. We wanted the highest possible hardness, so we embraced the "larger is truly better" philosophy when doing our analyses with the S/N ratio. In Table 6, there are the S/N ratios of microhardness of AA 8052 connections based on L9 orthogonal arrangement studies.

The optimum S/N and best microhardness values were achieved by utilizing a spinning speed of 1150 rpm, a travelling speed of 26 mm/min, and a cylinder pin with flutes as the device pin profile.

As can be seen in Figure 2, the S/N ratio of rotating speed declines between 950 rpm and 1450 rpm, making 950 rpm the optimal rotational speed with the highest S/N ratio. When travelling at a speed between 32.5 and 41 mm/min, the signal-to-noise ratio falls from 32.5 to 26. Thus, the ideal speed for travelling is 32.5 mm/min. The optimum resource pin account is CWF when the S/N ratio on the device pin profile page is cylindrical pin with flute to downside and then condensed from CWF to TRI.

3.6. Analysis of Variance. It is actually done to figure out how well certain process rules for microhardness work. In friction stir welding, the microhardness of welded 8052 aluminum joints is measured using an *F*-test to determine the relative importance of various parameters [26]. According to Table 7, each manageable parameter has a significant impact via pillar *F*.

Table 7 shows that travel speed accounts for 51.31% of the total, while rotational speed accounts for 34.23%. As a result, it is clear that the trip speed is more important than any other AA8052 alloy parameter for controlling residential properties such as microhardness since it pays the biggest dividends in achieving maximum microhardness.

3.7. Impact Strength. The Charpy test apparatus was employed to compute the impact strength of the AA8052 weld joints, and the findings are indicated in Table 8. Experiment 3 (950 rpm, 41 mm/min, TRI), test 5 (1150 rpm, 32.5 mm/min, Con), and practice 1 (950 rpm, 26 mm/min, CWF) showed that the greatest feasible impact strength was 7 J, while the lowest possible impact durability was 3.8 J.

3.8. Analysis of Sound-to-Noise Ratio. As a result of this investigation, influence strength was deemed to be one of the best symbolic buildings from which the guidelines for friction stir welding were optimized [27]. When using the S/N ratio, the "larger is actually better" approach was used since the maximum influence toughness was preferred. S/N ratios for friction stir bonded 8052 aluminum metals' joints depend on L9 orthogonal arrangement design and are shown in Table 9. The highest S/N market value was really 1150 rpm, 32.5 mm/min, and also downside with the most process conditions.

Spinning at 1150 rpm, travel at 32.5 mm/s, and a tool pin profile page for a conical cylinder pin were the perfect process specifications with the maximum S/N value (Con).

To summarize, the best rotational rate is 1400 rpm, which has the highest marketplace value, as the S/N ratio of rotating velocity rises from 950 rpm to 1450 rpm. Figure 3 shows the main effects plot on the S/N ratio. Trip velocity should be 41 mm/min because the sound-to-noise ratio of travelling velocity rises from 26 to 41 mm/min. S/N tool pin account ratios decline from CWT resources [28], improve from CWF resources, and then fall from TRI pin S/N ratios, as shown in Figure 3.

3.9. ANOVA. It is used to assess the impact strength of precise processing requirements on long-term toughness. Column F of Table 10 shows the % addition to each controllable constraint that has been found to have a substantial impact on the impact stamina of bonded AA 8052 joint in FSW.

According to Table 10, the tool pin geometry accounts of the total addition, while rotating speed subsidizes 4.29% and travel speed contributes 5.12% of the total contribution. Accordingly [29], the maneuver pin profile page demonstrates that the finest addition to obtaining extreme impact strength is the pin's position on the device.

Table 5: Results of the Vickers hardness test.

S. no	Rotational speed (W)	Travel speed (V)	Tool geometry	Vickers hardness number (HV)
1	950	26	CWF	116.35
2	950	32.5	Con	109.68
3	950	41	TRI	113
4	1150	26	CWF	117
5	1150	32.5	Con	116.35
6	1150	41	TRI	109.68
7	1450	26	CWF	113
8	1450	32.5	Con	117
9	1450	41	TRI	116.35

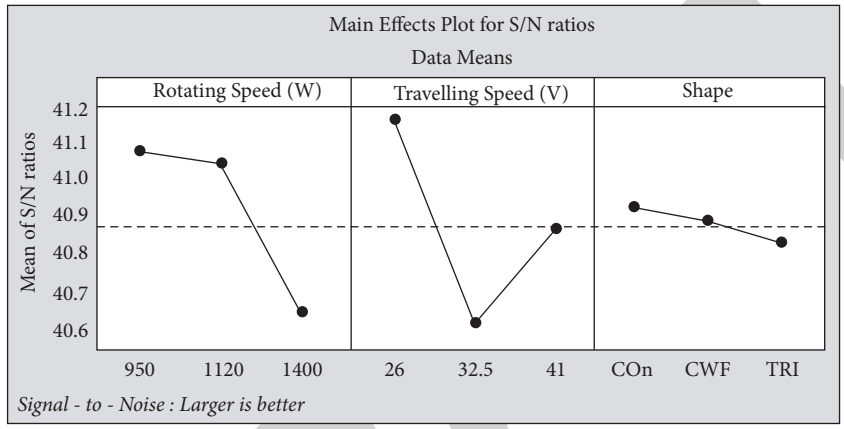

Figure 2: Main effects plot on sound-to-noise ratio.

Table 6: Sound-to-noise ratios of AA8052 joints.

S. no	Rotational speed (W)	Travel feed (V)	Tool pin geometry	Vickers hardness number (HV)	SN ratio
1	950	26	CWF	116.35	41.35
2	950	32.5	Con	109.68	40.82
3	950	41	TRI	113	40.80
4	1150	26	CWF	117	41.06
5	1150	32.5	Con	108	41.36
6	1150	41	TRI	112.67	40.69
7	1450	26	CWF	110.67	40.89
8	1450	32.5	Con	105	40.42
9	1450	41	TRI	108	40.67

Table 7: ANOVA for mean.

Source	DF	Adj SS	Adj MS	*F*-test	*P*
Rotating speed	2	0.2734	0.1367	34.15	0.029
Travelling speed	2	0.4103	0.2052	51.29	0.018
Tool pin profile	2	0.0047	0.0024	0.59	0.635
Error	2	0.0078	0.0040		
Total	8	0.6962			

Table 8: Impact strength test results.

S. no	Rotating speed (W)	Travelling speed (V)	Tool pin geometry	Impact strength (Joules)	S/N ratio
1	950	26.0	CWF	3.8	11.6581
2	950	32.5	Con	5	13.9429
3	950	41	TRI	7	16.6544
4	1150	26.0	CWF	5	13.7318
5	1150	32.5	Con	7	17.1980
6	1150	41.0	TRI	4.8	13.5793
7	1450	26.0	CWF	6.8	16.6047
8	1450	32.5	Con	5	13.7318
9	1450	41.0	TRI	5.6	15.2598

Table 9: S/N ratio of AA 8052 joints.

S. no	Rotating speed (W)	Travelling speed (V)	Tool pin geometry	Impact strength (Joules)	S/N ratio
1	950	26.0	CWF	3.7	11.6691
2	950	32.5	Con	5	13.9339
3	950	41	TRI	7	16.6544
4	1150	26.0	CWF	5	13.7318
5	1150	32.5	Con	7	17.1960
6	1150	41.0	TRI	4.8	13.5773
7	1450	26.0	CWF	6.8	16.6047
8	1450	32.5	Con	5	13.7318
9	1450	41.0	TRI	5.6	15.2598

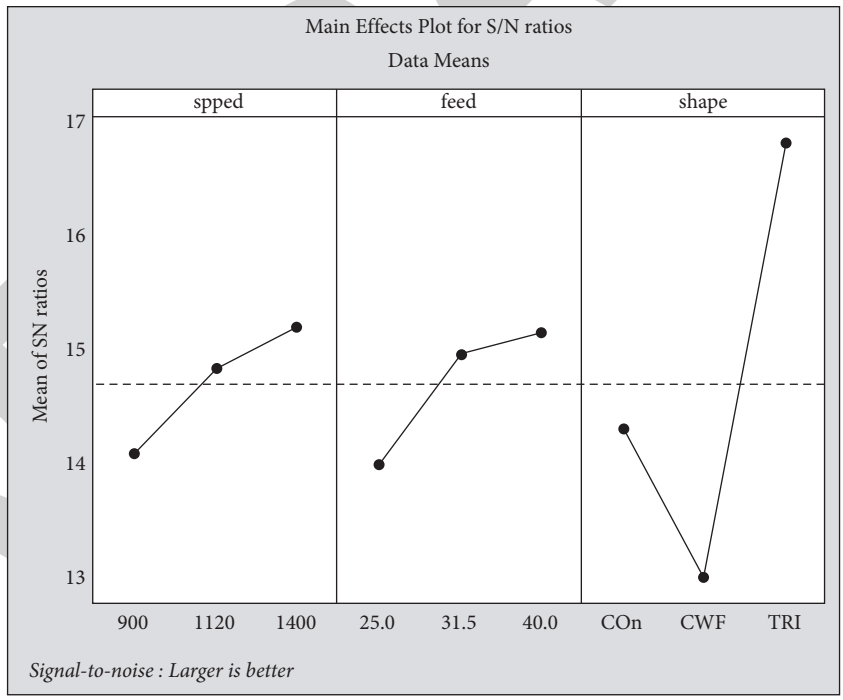

Figure 3: Main effects' plot on S/N ratio.

Table 10: ANOVA for mean.

Source	DF	Adj SS	Adj MS	*F*-test	*P*
Rotating speed	2	1.9447	0.9724	4.29	0.188
Travelling speed	2	2.3163	1.1582	5.12	0.165
Tool pin profile	2	22.6984	11.3493	50.10	0.021
Error	2	0.4532	0.2266		
Total	8	27.4124			

4. Conclusions

(i) Impact strength of AA8052 alloy joints can be measured using rotational speed, travel speed, and tool pin profile of 1150 rpm, 32.5 mm/min, and conical tool pins. These values were also found to be ideal for measuring ultimate tensile strength and microhardness. These conditions resulted in ultimate tensile strength and toughness measurements of 143.59 MPa and 117 J for the joint.

(ii) ANOVA was found to have a substantial impact on individual weld performance. It was found that the best technique parameters for maximum ultimate tensile strength were rotating speed of 1150 rpm, travel speed of 26 mm/min, and cylinder pin with flutes' tool profile (CWF). Rotating speed makes up 37.34% of the total ultimate tensile strength, while travel speed makes up 64.86%, tool pin profile makes up 1.154%, and so on. As a result, ultimate tensile strength is most strongly influenced by travel speed.

(iii) Rotating speed is 1150 rpm, travel speed is 26 mm/s, and tool pin profile is CWF, all of which work together to produce the highest possible microhardness. Rotational speed accounts for 34.23%, travel speed for 51.31%, and tool pin shape for 59% of the total contribution to achieving maximal microhardness. As a result, travel speed has a greater impact on microhardness than any other component.

(iv) Impact strength is best achieved with rotating speed of 1150 rpm, travel speed of 32.5 mm/s, and a tool pin profile with a concave cross section. Rotational speed contributes 43.9%, travel speed contributes 6.3%, and tool pin profile contributes 50.12% to achieving maximum impact strength.

(v) Thus, the tool pin profile has the greatest impact on the strength of the tool.

Data Availability

The data used to support the findings of this study are included within the article. Further data or information are available from the corresponding author upon request.

Conflicts of Interest

The authors declare that there are no conflicts of interest regarding the publication of this article.

Acknowledgments

The authors appreciate the supports from Arba Minch University, Ethiopia, for providing help during the research and preparation of the manuscript. The authors thank JECRC University, Rajkiya Engineering College, and S.A. Engineering College for providing assistance to complete this work.

References

[1] N. Abdulwadood, B. Sahin, and N. Yildirim, "Effect of welding parameters on the mechanical properties of dissimilar aluminum alloys 2024-T3 to 6061-T6 joints produced by friction stir welding," *Nigde Univ. Muhendis. Bilim. Degisti*, vol. 3, pp. 1–11, 2012.

[2] D. K. Rajendran, G. B. Kannan, and S. Muthukumaran, "Investigation on the mechanical and wear properties of aluminium-magneisum bimetallic composite fabricated by friction stir processing technique," *Transactions of the Indian Institute of Metals*, vol. 71, no. 5, pp. 1247–1255, 2018.

[3] Y. Zhang, Y. Chen, D. Yu, D. Sun, and H. Li, "A review paper on effect of the welding process of ceramics and metals," *Journal of Materials Research and Technology*, vol. 9, no. 6, ISSN 2238-7854, Article ID 16236, 2020.

[4] V. Mohanavel, M. Ravichandran, and S. Suresh Kumar, "Optimization of tungsten inert gas welding parameters to," *Materials Today Proceedings*, vol. 5, no. 11, pp. 25112–25120, 2018, Part 3.

[5] X. Wang, K. Wang, Y. Shen, and K. Hu, "Comparison of fatigue property between friction stir and TIG welds," *Journal of University of Science and Technology Beijing Mineral Metallurgy, Material*, vol. 15, no. 3, pp. 280–284, 2008.

[6] K. Mariyappan, K. Praveen, S. S. Kumar, K. Kadambanathan, S. Rajamanickam, and R. Vignesh, "Characterization of brass/steel plates joined by friction stir welding," *International Journal of Engineering & Technology*, vol. 7, no. 3, pp. 366–368, 2018.

[7] F. Gharavi, K. A. Matori, R. Yunus, and N. K. Othman, "Corrosion behavior of friction stir welded lap joints of AA6061-T6 aluminum alloy," *Materials Research*, vol. 17, no. 3, pp. 672–681, 2014.

[8] G. N. ShivaKumar and G. Rajamurugan, "Friction stir welding of dissimilar alloy combinations-a review," *Proceedings of the Institution of Mechanical Engineers - Part C: Journal of Mechanical Engineering Science*, vol. 2022, Article ID 095440622110, 2022.

[9] M. M. Moradi, H. Jamshidi Aval, R. Jamaati, S. Amirkhanlou, and S. Ji, "Microstructure and texture evolution of friction stir welded dissimilar aluminum alloys: AA2024 and AA6061," *Journal of Manufacturing Processes*, vol. 32, pp. 1–10, 2018.

[10] V. K. S. Jain, J. Varghese, S. Muthukumaran, and S. Muthukumaran, "Effect of first and second passes on microstructure and wear properties of titanium dioxide-reinforced aluminum surface composite via friction stir processing," *Arabian Journal for Science and Engineering*, vol. 44, no. 2, pp. 949–957, 2018.

[11] V. S. Gaikwad and S. Chinchanikar, "Mechanical behaviour of friction stir welded AA7075-T651 joints considering the effect of tool geometry and process parameters," *Advances in Materials and Processing Technologies*, vol. 2021, pp. 1–19, 2021.

[12] G. Rambabu, D. Balaji Naik, C. H. Venkata Rao, K. Srinivasa Rao, and G. Madhusudan Reddy, "Optimization of friction stir welding parameters for improved corrosion resistance of AA2219 aluminum alloy joints," *Defence Technology*, vol. 11, no. 4, pp. 330–337, 2015.

[13] A. Boşneag, M. A. Constantin, E. Niţu, and M. Iordache, "Friction Stir Welding of three dissimilar aluminium alloy used in aeronautics industry," *IOP Conference Series: Materials Science and Engineering*, vol. 252, no. 1, Article ID 012041, 2017.

[14] R. P. Matrukanitz, "Selection and weldability of heat-treatable aluminum alloys," *ASM Handbook-Welding, Brazing Solder*, vol. 6, pp. 528–536, 1990.
[15] Y. S. Sato, P. Arkom, H. Kokawa, T. W. Nelson, and R. J. Steel, "Effect of microstructure on properties of friction stir welded Inconel Alloy 600," *Materials Science and Engineering A*, vol. 477, no. 1-2, pp. 250–258, 2008.
[16] C. Blignault, D. G. Hattingh, G. H. Kruger, T. I. van Niekerk, and M. N. James, "Friction stir weld process evaluation by multi-axial transducer," *Measurement*, vol. 41, no. 1, pp. 32–43, 2008.
[17] Z. W. Chen, T. Pasang, and Y. Qi, "Shear flow and formation of Nugget zone during friction stir welding of aluminium alloy 5083-O," *Materials Science and Engineering A*, vol. 474, no. 1-2, pp. 312–316, 2008.
[18] W. M. Thomas and E. D. Nicholas, "Friction stir welding for the transportation industries," *Materials & Design*, vol. 18, no. 4–6, pp. 269–273, 1997.
[19] Z. Zhang and H. W. Zhang, "Numerical studies on controlling of process parameters in friction stir welding," *Journal of Materials Processing Technology*, vol. 209, no. 1, pp. 241–270, 2009.
[20] P. Cavaliere, G. Campanile, F. Panella, and A. Squillace, "Effect of welding parameters on mechanical and microstructural properties of AA6056 joints produced by Friction Stir Welding," *Journal of Materials Processing Technology*, vol. 180, no. 1-3, pp. 263–270, 2006.
[21] S. Nansaarng and K. Chaivanich, *A Research Study of the Impact of Specifications of Diverse Components Signing up with on Abrasion Rouse Assembly Procedure Deliberately of Speculative*, Fifth Glob. Meet. Warmth Trans, Athens, Greece, 2007.
[22] T. Azimzadegan and S. Serajzadeh, "An investigation into microstructures and mechanical properties of AA7075-T6 during friction stir welding at relatively high rotational speeds," *Journal of Materials Engineering and Performance*, vol. 19, no. 9, pp. 1256–1263, 2010.
[23] M. Nourani, A. S. Milani, and S. Yannacopoulos, "Taguchi optimization of process parameters in friction stir welding of 6061 aluminum alloy: a review and case study," *Engineering*, vol. 03, no. 02, pp. 144–155, 2011.
[24] A. Kamyabi-Gol and M. Sheikh-Amiri, "Spheroidizing kinetics and optimization of heat treatment parameters in CK60 steel using Taguchi robust design," *Journal of Iron and Steel Research International*, vol. 17, no. 4, pp. 45–52, 2010.
[25] E. M. Anawa and A. G. Olabi, "Using Taguchi method to optimize welding pool of dissimilar laser-welded components," *Optics & Laser Technology*, vol. 40, no. 2, pp. 379–388, 2008.
[26] R. K. Roy, *A Primer on the Taguchi Method*, The University of California, Oakland, CA, USA, 1990.
[27] E. Taban and E. Kaluc, "Microstructural and mechanical properties of double-sided MIG, TIG and friction stir welded 5083-H321 aluminium alloy," *Kov. Mater.*vol. 44, no. 1, p. 25, 2006.
[28] M. Jayaraman, R. Sivasubramanian, V. Balasubramanian, and A. K. Lakshminarayanan, "Optimization of process parameters for friction stir welding of cast aluminium alloy A319," *by Taguchi Method*, vol. 68, no. 1, pp. 36–43, 2009.
[29] A. K. Lakshminarayanan and V. Balasubramanian, "Process parameters optimization for friction stir welding of RDE-40 aluminium alloy using Taguchi technique," *Transactions of Nonferrous Metals Society of China*, vol. 18, no. 3, pp. 548–554, 2008.